NACA RM L55L19b

NACA

RESEARCH MEMORANDUM

AERODYNAMIC HEATING OF AIRCRAFT COMPONENTS

By Leo T. Chauvin

Langley Aeronautical Laboratory
Langley Field, Va.

NATIONAL ADVISORY COMMITTEE
FOR AERONAUTICS

WASHINGTON
February 14, 1956
Declassified January 12, 1961

NATIONAL ADVISORY COMMITTEE FOR AERONAUTICS

RESEARCH MEMORANDUM

AERODYNAMIC HEATING OF AIRCRAFT COMPONENTS

By Leo T. Chauvin

SUMMARY

Aerodynamic heat-transfer data obtained at supersonic speeds are presented for various airplane components such as a conical nose, a blunt conical nose, a cone-cylinder body, a flat-faced canopy, a delta wing at angle of attack, and a deflected flap. The data are correlated on the basis of Stanton number for various supersonic Mach numbers and Reynolds numbers.

For all cases investigated, measurements were in reasonable agreement with theoretical predictions, except for the sheltered surface of the delta wing at angle of attack.

In addition to the heat transfer measured on the 50° blunt cone, transition was found to occur at a transition Reynolds number of 0.5×10^6 based on local conditions at a free-stream Mach number of 4.84.

INTRODUCTION

The designer of the supersonic airplane is confronted with the analysis of various airplane components for aerodynamic heating. Inasmuch as most heating data have been for very simple shapes, the importance of detail design may easily be missed. Recently, large-scale heat transfer data have been obtained from free-flight and free-jet tests of such airplane components as blunt noses, canopies, wings at angle of attack, and deflected control flaps. The purpose of this paper is to review new and significant data which will be of interest to designers in determining the heating of these components. A comparison with existing theory to indicate its adequacy in each case is also presented.

SYMBOLS

M	Mach number
R	Reynolds number

N_{St} Stanton number, $h/c_p\rho V$

h local aerodynamic heat-transfer coefficient, $\frac{\text{Btu}}{(\text{sec})(\text{sq ft})(^{\circ}\text{F})}$

c_p specific heat of air at constant pressure, $\frac{\text{Btu/slug}}{^{\circ}\text{F}}$

ρ density of air, slugs/cu ft

V velocity, ft/sec

x distance along model surface, ft or in. as indicated

α angle of attack, deg

δ control deflection, deg

T temperature, $^{\circ}$F or $^{\circ}$F abs

Subscripts:

l outside the boundary layer

T transition

W conditions pertaining to the skin of model

∞ free stream

AIRPLANE COMPONENTS

A breakdown of the various components of the airplane for which heat-transfer data are available is presented in the following table:

Nose: cone, circular arc, parabola, hemisphere, Von Kármán
Body: cylinder, cone cylinder, hemispherical-nose cylinder, parabola
Canopy: flat-faced canopy
Wing: plan form: unswept, delta
Control: sealed flap

As can be seen, data are available for a wide range of nose shapes and bodies; whereas information is limited to only one canopy shape, two wing plan forms, and one flap arrangement. Information for some of the listed components can be found in references 1 to 12.

Nose and Body

In order to investigate heat transfer on a simple nose shape at high Reynolds number, flight tests were made on a large 10° cone. This test model, shown in figure 1, had an 18-inch base and was 7.5 feet long. The model was rocket launched at low altitude, which for $M_l = 3$ gave a Reynolds number per foot of 18×10^6, or 135×10^6 based on the full cone length. In order to keep a low skin temperature favorable for laminar flow, the skin was made of 0.08-inch copper and the model was accelerated rapidly.

The thermocouple locations are indicated on the sketch shown in figure 1. The skin temperature and Stanton number are shown plotted against body length. Note that the maximum temperature was obtained about 2 feet back from the nose tip and this result indicates that transition to turbulent flow had taken place. The condition of the boundary layer is shown more clearly by the heat-transfer data in the lower part of the figure plotted as local Stanton number. The data show laminar heat transfer for the forward part of the nose, with transition occurring at 1.85 feet from the nose tip at a Reynolds number of 33×10^6. The measured heat-transfer coefficients for the laminar region agree well with the theory of reference 13. For the turbulent region, the theory of reference 14 is in good agreement when the characteristic length for the theory is the length behind the transition point. This agreement is quite significant in view of the rather large longitudinal temperature gradient that existed when the measurements were made and the fact that the theory assumes constant wall temperature.

A large amount of large-scale data are available for parabolic noses and complete bodies such as the NACA RM-10 missile. For a cone-cylinder body, however, only recently have large-scale data been obtained at high Mach numbers. A part of these new data are shown in figure 2. A 15° conical nose on an 8.5-inch-diameter cylinder was flown to a Mach number of approximately 5. The heat-transfer data are presented as a function of body length for two flight conditions. For $M_l = 4.5$ and R_l per foot of 5.5×10^6, the data on the nose are laminar and agree with theory (ref. 13); transition occurs shortly after the cone-cylinder juncture and is spread over a wide region. The data rearward of the transition region are in agreement with turbulent theory (ref. 14). For $M_l = 3.0$ and R_l per foot of 16.4×10^6, turbulent heat transfer existed at all measurement stations and is in good agreement with theory except for the cylindrical section where the data are lower than the theoretical results. The theory for this case overestimates the value for the heat transfer.

In view of the interest in blunt noses for radomes and, in particular, to avoid the high heating rate on the extreme point, a large blunted cone

has been flight tested to a Mach number of 5. This nose as shown in figure 3 had a 50° total angle with a base diameter of approximately 18 inches and a nose diameter one-half this value. Both temperatures and pressures were measured at the station shown. Figure 3 gives the measured wall temperature plotted against length from the stagnation point in inches for $M_\infty = 4.84$ as the model accelerated to $M_\infty = 5$. The Reynolds number based on free-stream conditions was 22.4×10^6 per foot. The temperature data indicate that transition started at approximately 2 inches from the stagnation point or at approximately 30° corresponding to $R_\infty = 3 \times 10^6$. Converting this transition Reynolds number to local conditions yields a value of only 0.5×10^6, even though the local temperature ratio was only 0.48. Measured heat-transfer coefficients are shown plotted as a function of distance from the stagnation point. At the stagnation point, the theory of Sibulkin (ref. 15) is in good agreement with the experiment, whereas for the rearmost station on the cone the data are approximately 10 percent lower than the theory for turbulent cones when the theory is based on the distance from the transition point. It is evident from these data that this nose shape poses a severe heating problem because of the unexpected early transition.

Canopy

A very important component of the airplane for which the design requires large-scale heat-transfer data is the canopy. Heat transfer on a typical flat-faced canopy has been recently measured from a flight test and is shown in figure 4. The canopy was located 4 feet back of the nose of a parabolic body 12.5 feet long. The flat windshield was sweptback 63°. The heat transfer measured at $M_\infty = 3.0$, $R_\infty = 13 \times 10^6$ per foot is presented as a function of canopy length; also shown as a dashed curve is heat transfer on the basic body. It can be seen that the heat transfer on the face of the canopy is more than twice that on the basic parabolic body. The heat transfer on the rear of the canopy is considerably less than the corresponding heat transfer on the basic body. Two-dimensional shock theory was used for the local conditions on the windshield, and the theory (ref. 14) based on these local conditions is in fair agreement with the heat-transfer measurements. Theoretical heat-transfer coefficients calculated for the rear of the canopy by use of Prandtl-Meyer expansions for the local conditions are somewhat higher than the measurements.

Wing and Controls

Consideration is next given to the possibilities of computing the heat transfer on typical wings and controls. Figure 5 shows typical

aerodynamic heat-transfer coefficients obtained on a 60° delta wing of NACA 65A005 section. The tests were made in a free jet at $M_\infty = 2.0$ and Reynolds number of 14×10^6 per foot. In order to minimize the thermal stresses normally encountered in this type of test, the wing skin was constructed from 0.032-inch Invar, which has a low coefficient of thermal expansion. The Stanton number is shown plotted against distance in percent chord for angles of attack of 0°, 3°, and 6°. Turbulent flow is indicated by the heat-transfer data at all stations. The Reynolds number at the forward station was 5×10^6. The data show that, for the lower surface, increasing α to 6° caused approximately a 15-percent increase in the heat-transfer coefficient, whereas for the upper surface the heat-transfer coefficient is approximately 15 percent lower for $\alpha = 3°$ and approximately 30 percent lower for $\alpha = 6°$.

In order to indicate the possibility of predicting the heat transfer from theory, the heat-transfer coefficients on the wing from figure 5 are replotted in figure 6, together with data at $\alpha = 9°$. These data are correlated as the ratio of experimental Stanton number to theoretical Stanton number (ref. 14), where the parameters are based on local conditions in which the length factor is the distance from the leading edge to the measurement stations. The data are plotted against distance in percent chord. Perfect agreement with theory is a ratio of 1.0. The chart shows good correlation at all angles of attack on the lower surface, whereas on the upper surface good correlation is obtained only at $\alpha = 3°$. At $\alpha = 6°$, the experimental data give a heating rate only 78 percent of that predicted by theory and at $\alpha = 9°$ the experimental values are 65 percent of the theoretical values. This difference is believed to be due to separation at the higher angles of attack.

Heat transfer to a deflected control surface is presented in figure 7. The data are for a flap control of the sealed type extending across the trailing edge of a delta wing. Data were obtained from flight tests as the model accelerated to $M_\infty = 2.7$. The model had four wings in a cruciform arrangement with controls deflected like ailerons. Two opposing flaps were deflected 10° and the other two were deflected 20° in a direction to oppose the roll of the first two. As a result, a small rate of roll remained, which induced an angle of attack at the measuring station of less than 1°. The Stanton number based on free-stream conditions is plotted against flight Mach number for a midspan station near the trailing edge. The Reynolds number was approximately 9×10^6 per foot. The filled-in symbols are for the lower surface and the open symbols for the upper surface of the flap. The data for the lower surface with the 20° deflection are approximately 4 times those of the upper surface for all Mach numbers, and 2.5 times those of the upper surface for the 10° deflection.

A comparison with theory at $M_\infty = 2.64$ and a flap deflection of 10° is presented in figure 8. Stanton number is plotted against chord length

for two measurement stations on the flap and one station on the wing ahead of the flap. The data are in good agreement with theory (ref. 14) for a deflected plate based on the length from the leading edge of the wing.

CONCLUDING REMARKS

The heat transfer obtained in supersonic flight tests for a conical nose, a blunt conical nose, a cone-cylinder body, a flat-faced canopy, and a deflected flap has been experimentally measured. For a delta wing, data were obtained in a blowdown-type jet at a Mach number of 2.0 for various angles of attack.

Early transition was obtained from the flight test of the 50° blunt cone at a Mach number of 4.84 and a Reynolds number (per foot) of 22.4×10^6 based on free-stream conditions. Transition from laminar to turbulent boundary layer occurred at 1.5 inches from the stagnation point corresponding to a Reynolds number of 0.5×10^6 based on local conditions. The theory of Sibulkin for the stagnation-point heat transfer was in good agreement with the measurements.

The heat-transfer data for the various components investigated were in good agreement with the predicted heat transfer except for the sheltered surface of the delta wing at angle of attack.

Langley Aeronautical Laboratory,
National Advisory Committee for Aeronautics,
Langley Field, Va., November 3, 1955.

REFERENCES

1. Rumsey, Charles B., Piland, Robert O., and Hopko, Russel N.: Aerodynamic-Heating Data Obtained From Free-Flight Tests Between Mach Numbers of 1 and 5. NACA RM L55A14a, 1955.

2. Rumsey, Charles B.: Free-Flight Measurements of Aerodynamic Heat Transfer to Mach Number of 3.9 and of Drag to Mach Number 6.9 of a Fin-Stabilized Cone-Cylinder Configuration. NACA RM L55G28a, 1955.

3. Rabb, Leonard, and Simpkinson, Scott H.: Free-Flight Heat-Transfer Measurements on Two 20° Cone-Cylinders at Mach Numbers From 1.3 to 4.9. NACA RM E55F27, 1955.

4. Messing, Wesley E., Rabb, Leonard, and Disher, John H.: Preliminary Drag and Heat-Transfer Data Obtained From Air-Launched Cone-Cylinder Test Vehicle Over Mach Number Range From 1.5 to 5.18. NACA RM E53I04, 1953.

5. Scherrer, Richard: Comparison of Theoretical and Experimental Heat Transfer Characteristics of Bodies of Revolution at Supersonic Speeds. NACA Rep. 1055, 1951. (Supersedes NACA RM A8L28 by Scherrer, Wimbrow, and Gowen; NACA TN 1975 by Wimbrow; NACA TN 2087 by Scherrer and Gowen; NACA TN 2131 by Scherrer; and NACA TN 2148 by Wimbrow and Scherrer.)

6. Chauvin, Leo T., and Maloney, Joseph P.: Turbulent Convective Heat-Transfer Coefficients Measured From Flight Tests of Four Research Models (NACA RM-10) at Mach Numbers From 1.0 to 3.6. NACA RM L54L15, 1955.

7. Piland, Robert O., and Collie, Katherine A.: Aerodynamic Heating of Rocket-Powered Research Vehicles at Hypersonic Speeds. NACA RM L55E10c, 1955.

8. Sommer, Simon C., and Short, Barbara J.: Free-Flight Measurements of Turbulent-Boundary-Layer Skin Friction in the Presence of Severe Aerodynamic Heating at Mach Numbers from 2.8 to 7.0. NACA TN 3391, 1955.

9. Chauvin, Leo T., and Maloney, Joseph P.: Experimental Convective Heat Transfer to a 4-Inch and 6-Inch Hemisphere at Mach Numbers From 1.62 to 3.04. NACA RM L53L08a, 1954.

10. Stine, Howard A., and Wanlass, Kent: Theoretical and Experimental Investigation of Aerodynamic-Heating and Isothermal Heat-Transfer Parameters on a Hemispherical Nose With Laminar Boundary Layer at Supersonic Mach Numbers. NACA TN 3344, 1954.

11. Korobkin, Irving: Laminar Heat Transfer Characteristics of a Hemisphere for the Mach Number Range 1.9 to 4.9. NAVORD Rep. 3841 (Aeroballistic Res. Rep. 257), U. S. Naval Ord. Lab. (White Oak, Md.), Oct. 10, 1954.

12. Jones, Ira P., Jr.: Measurements of Aerodynamic Heating Obtained During Demonstration Flight Tests of the Douglas D-558-II Airplane. NACA RM L52I26a, 1952.

13. Van Driest, E. R.: Investigation of Laminar Boundary Layer in Compressible Fluids Using the Crocco Method. NACA TN 2597, 1952.

14. Van Driest, E. R.: Turbulent Boundary Layer in Compressible Fluids. Jour. Aero. Sci., vol. 18, no. 3, Mar. 1951, pp. 145-160, 216.

15. Sibulkin, M.: Heat Transfers Near the Forward Stagnation Point of a Body of Revolution. Jour. Aero. Sci. (Readers' Forum), vol. 19, no. 8, Aug. 1952, pp. 570-571.

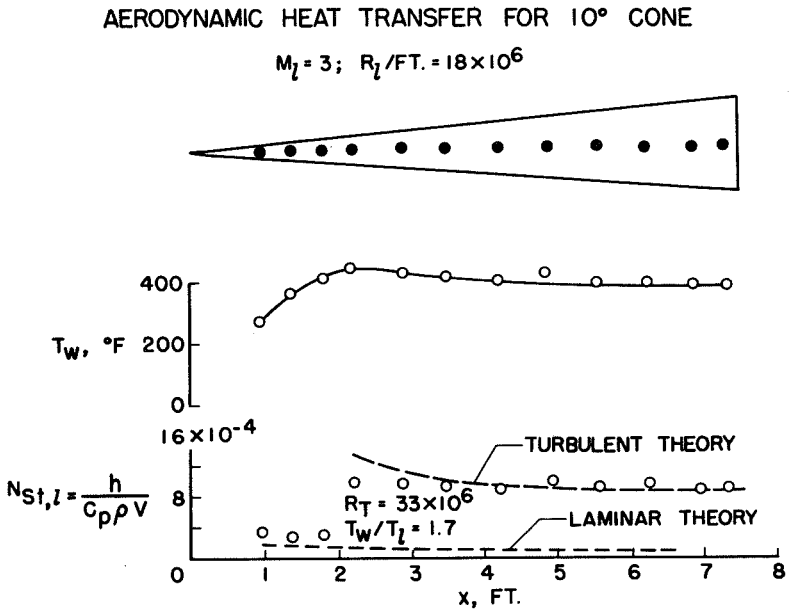

Figure 1

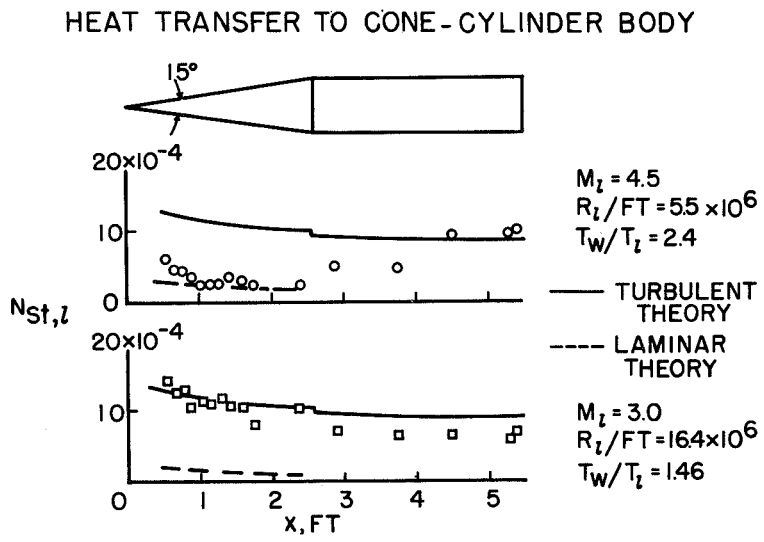

Figure 2

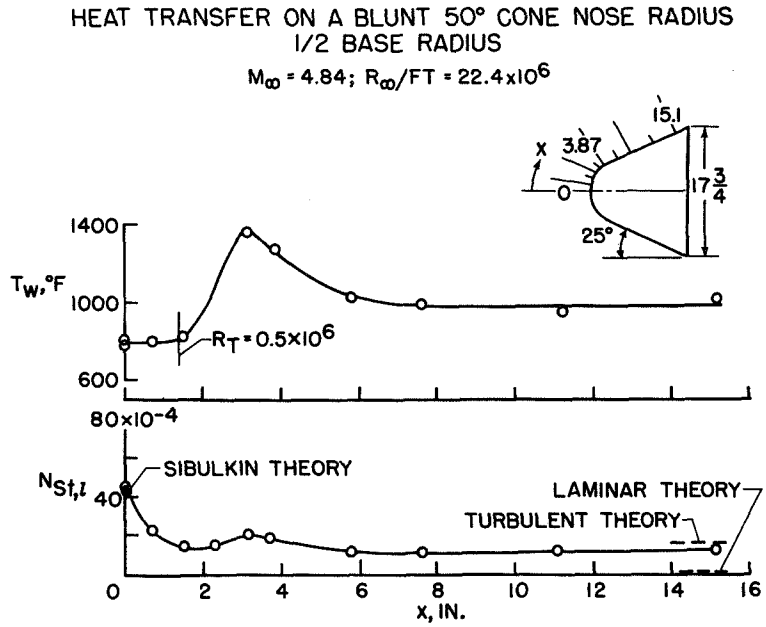

Figure 3

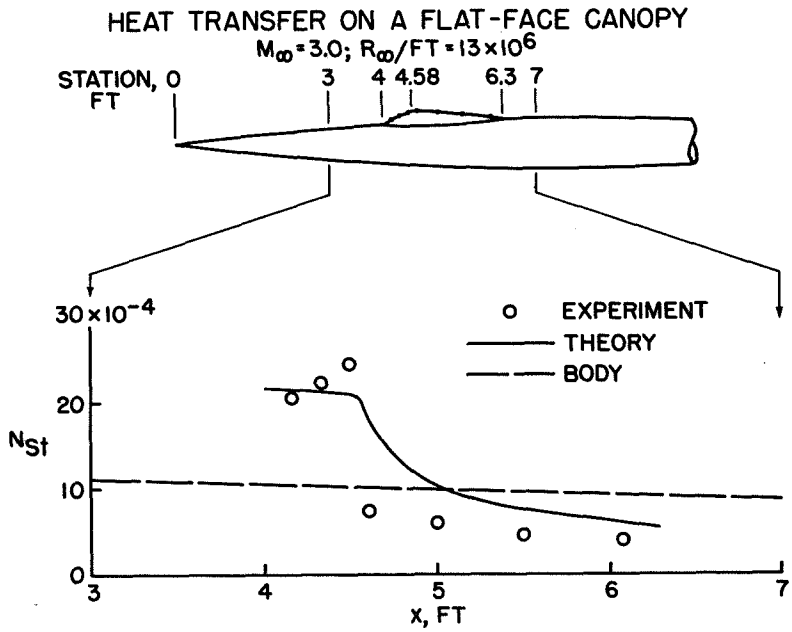

Figure 4

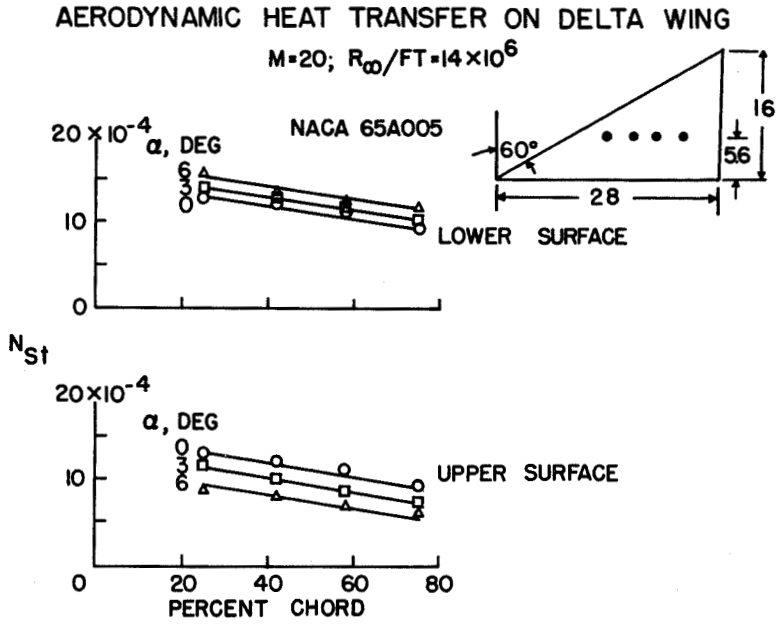

Figure 5

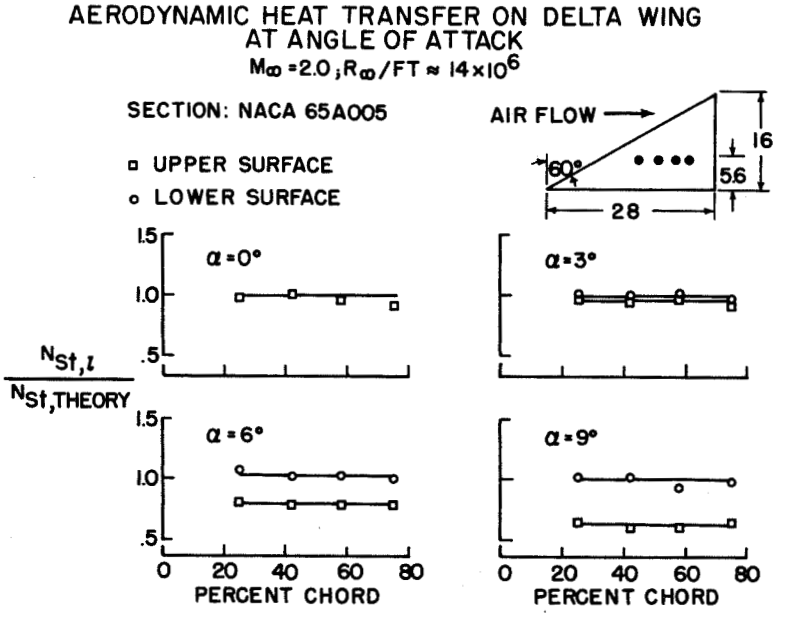

Figure 6

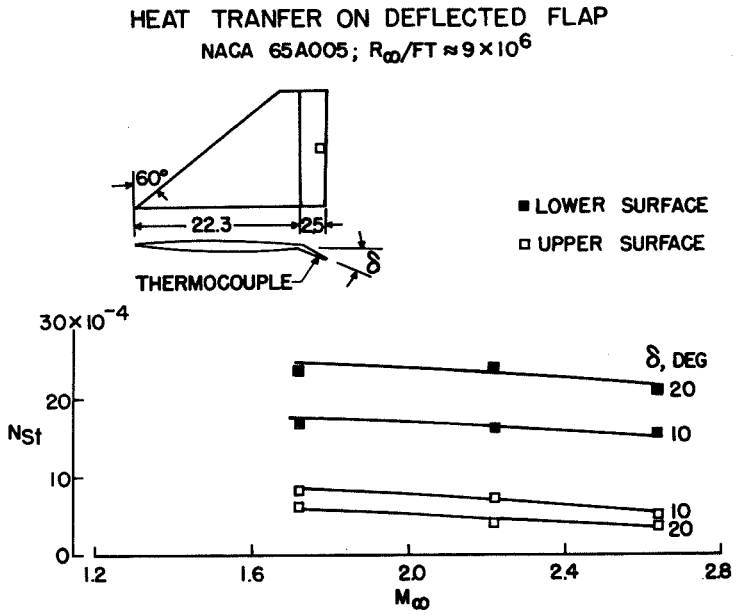

Figure 7

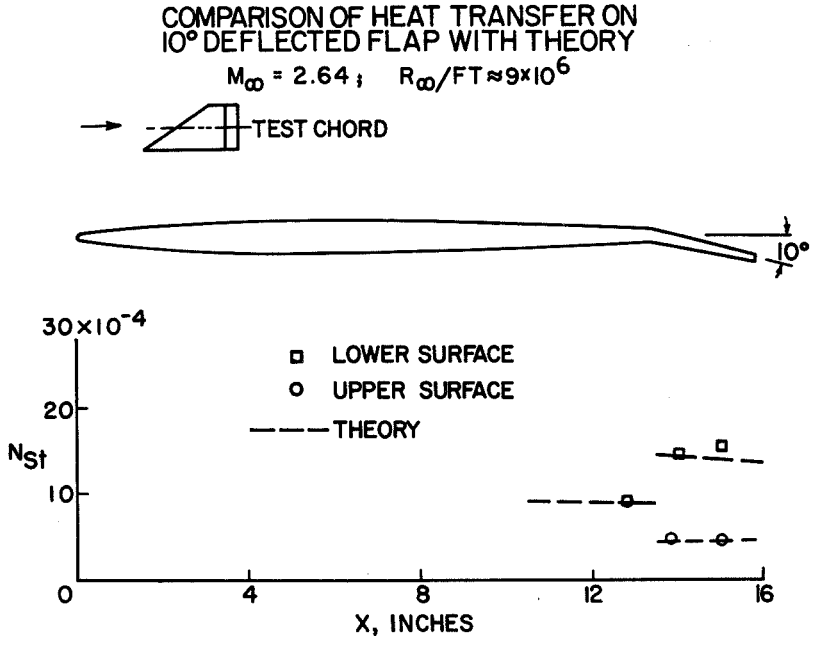

Figure 8